DNS of convective heat transfer in a rotating cylinder

DNS of Convective Heat Transfer in a Rotating Cylinder

R.P.J. Kunnen[1,2], B.J. Geurts[1,3], and H.J.H. Clercx[1,3]

[1] Department of Applied Physics and J.M. Burgers Centre for Fluid Dynamics, Eindhoven University of Technology, P.O. Box 513, 5600 MB Eindhoven, The Netherlands, b.j.geurts@utwente.nl; h.j.h.clercx@tue.nl

[2] Current address: RWTH Aachen University, Institute of Aerodynamics, Wüllnerstraße 5a, 52062 Aachen, Germany, R.Kunnen@aia.rwth-aachen.de

[3] Department of Applied Mathematics and J.M. Burgers Centre for Fluid Dynamics, University of Twente, P.O. Box 217, 7500 AE Enschede, The Netherlands

Abstract The effects of rotation on the convective heat transfer and flow structuring in a cylindrical volume of fluid is investigated with direct numerical simulation (DNS). A formulation of the discrete equations of motion in cylindrical coordinates is solved with finite-difference approximations. At constant Rayleigh (Ra; dimensionless temperature gradient) and Prandtl (σ; characterises diffusive properties of the fluid) numbers, the Rossby number Ro, the ratio of buoyancy and Coriolis forces, is varied between runs with $0.045 \leq Ro \leq \infty$. For $Ro \gtrsim 1.2$ we find the so-called large-scale circulation. At $Ro \lesssim 1.2$ slender columnar vortical plumes are found. In a range of Ro heat transfer is increased by Ekman pumping in the vortical plumes.

1 Introduction

Large-scale geophysical flows, as found in the atmosphere and in the oceans, are often driven by buoyancy, and subsequently shaped by the rotation of our Earth through the Coriolis force. Similar conditions can be found in the convective layer in the Sun and inside the giant planets. Next to fundamental interest, rotating convection is a relevant topic in meteorology, climatology, oceanography and astrophysics.

We approximate these complicated flows by a simple model. A cylindrical volume of fluid is heated from below, cooled from above, and subjected to a rotation with orientation parallel to the cylinder axis and counter to gravity. The destabilising temperature gradient is designated in dimensionless form by the Rayleigh number Ra. The rotation rate is specified by the Taylor number Ta. The diffusive properties of the fluid are characterised by the Prandtl number σ. These numbers are defined as

V. Armenio et al. (eds.), *Direct and Large-Eddy Simulation VII*, ERCOFTAC Series 13, DOI 10.1007/978-90-481-3652-0_56,

$$Ra \equiv \frac{g\alpha \Delta T H^3}{\nu\kappa}\,, \quad Ta \equiv \left(\frac{2\Omega H^2}{\nu}\right)^2\,, \quad \sigma \equiv \frac{\nu}{\kappa}\,, \tag{1}$$

with H the vertical separation of the plates and ΔT the temperature difference between them, g the gravitational acceleration, Ω the rotation rate, and ν, κ and α the kinematic viscosity, thermal diffusivity and thermal expansion coefficient of the fluid, respectively. The cylindrical domain adds a fourth parameter, the diameter-to-height aspect ratio Γ, which in this study is set to one. Another useful definition is the Rossby number $Ro = \sqrt{Ra/(\sigma Ta)}$ as a direct indication of the ratio of buoyancy over Coriolis forces. An important result in convection, the heat transfer, is commonly expressed in dimensionless form as the Nusselt number Nu, the convective heat transfer normalised by the conductive part of the heat flux.

A cylindrical geometry is the default choice for experimental investigations. It also adds a phenomenon of fundamental interest: the organisation of the motion into a domain-filling large-scale circulation (LSC). In non-rotating cylindrical convection the LSC has received considerable attention (see, e.g., Refs. [1,2]). It is the starting point of theories [3] that describe the convective heat transfer as a function of Ra and σ. Rotation adds interesting temporal dynamics in the LSC [4]. It is found that at a certain rotation rate the LSC is no longer present; instead an array of strongly localised vertical vortices is found, transporting fluid and heat vertically [5].

We study rotating convection in a cylinder with direct numerical simulation (DNS) at constant Ra and σ, where the rotation rate is varied between runs. The following topics will be addressed: (i) the persistence of the LSC under rotation [4], (ii) the organisation of the flow in the vortical state at higher rotation rates [5], and (iii) the convective heat flux (Nu) as a function of Ro [6,7]. These results reinforce some of our recent experimental findings [8] found using stereoscopic particle image velocimetry in turbulent rotating convection.

2 Numerical procedure

The governing equations are the incompressible Navier–Stokes and temperature equations, written in the Boussinesq approximation [9] with the Coriolis term added:

$$\begin{aligned} \frac{\partial \mathbf{u}}{\partial t} + (\mathbf{u}\cdot\boldsymbol{\nabla})\mathbf{u} + \frac{1}{Ro}\hat{\mathbf{z}}\times\mathbf{u} &= -\boldsymbol{\nabla}p + \sqrt{\frac{\sigma}{Ra}}\nabla^2\mathbf{u} + T\hat{\mathbf{z}}\,, \\ \frac{\partial T}{\partial t} + (\mathbf{u}\cdot\boldsymbol{\nabla})T &= \frac{1}{\sqrt{\sigma Ra}}\nabla^2 T\,, \\ \boldsymbol{\nabla}\cdot\mathbf{u} &= 0\,, \end{aligned} \tag{2}$$

where $\mathbf{u}$ is the (co-rotating) velocity vector, p the reduced pressure, and T the temperature relative to the cold top wall. Velocities are scaled with the so-called free-fall velocity $U \equiv \sqrt{g\alpha \Delta T H}$ [10], lengths are scaled with height H, and the temperature with ΔT. The boundary conditions for velocity are no-slip on all walls. The sidewall is thermally insulating (zero temperature gradient) while the bottom and top walls are isothermal: $T = 0$ at the top and $T = 1$ at the bottom wall.

The solution to the Navier–Stokes equations in cylindrical coordinates provides some challenges, like the treatment of the equations on the cylinder axis $r = 0$. The discretisation proposed by Verzicco and Orlandi [11] treats the singularity by writing the equations in terms of u_ϕ, $q_r = r\, u_r$ and u_z, with u_ϕ, u_r and u_z the azimuthal, radial and axial velocity component, respectively. The finite-difference discretisation on a staggered mesh is second-order accurate. Time advancement is done using a third-order Runge–Kutta scheme with an adaptive time step. For further details on the numerical procedure we refer to Verzicco and Camussi [10] and Verzicco and Orlandi [11].

The simulations are carried out at constant $Ra = 1 \times 10^9$ and $\sigma = 6.4$, corresponding to strongly turbulent convection in water. The Rossby number takes values between ∞ (no rotation) and 0.045 (strong rotation). The grid resolution is set to $385 \times 193 \times 385$ for the azimuthal, radial and axial directions, respectively. Near the bottom and top walls, as near the sidewall, the grid spacing decreases to cluster more grid points in the boundary layers. In the most demanding case, $Ro = 0.045$, there are 8 grid points in the sidewall boundary layer and 10 in the layers near bottom and top. Averaging was done for at least 150 large-eddy turnover times, tested separately and found to yield accurate results for approximating the long-time averages. Furthermore, 64 numerical probes placed at half-height are distributed evenly over a circle at $r = 0.45$ close to the sidewall ($r = 0.5$). At these points, local time histories of velocity, temperature, and other quantities are recorded, to be used momentarily in the analysis of the LSC.

3 Coherent structures in the flow

The variations in flow structuring due to rotation are shown in Fig. 1. Three cases are included: (a) no rotation $Ro = \infty$, (b) medium rotation $Ro = 0.72$, and (c) strong rotation $Ro = 0.045$. In plot (a) at $Ro = \infty$ isosurfaces of vertical velocity are plotted: dark (light) colouring corresponds to upward (downward) flow. A spatial separation of upward and downward flow is observed, a fingerprint of the LSC. In (b,c) isosurfaces of the so-called Q criterion for the detection of vortices are plotted [12]:

$$Q \equiv \frac{1}{2}\left(\left\| \boldsymbol{\nabla}\mathbf{u} - (\boldsymbol{\nabla}\mathbf{u})^T \right\|^2 - \left\| \boldsymbol{\nabla}\mathbf{u} + (\boldsymbol{\nabla}\mathbf{u})^T \right\|^2 \right) .$$

Q is positive when the antisymmetric (rotational) part of $\boldsymbol{\nabla}\mathbf{u}$ dominates over the symmetric (strain) part, i.e., inside a vortex. At $Ro = 0.72$ (b) there is no LSC; a few coherent vortices can be found. At $Ro = 0.045$ (c) many slender

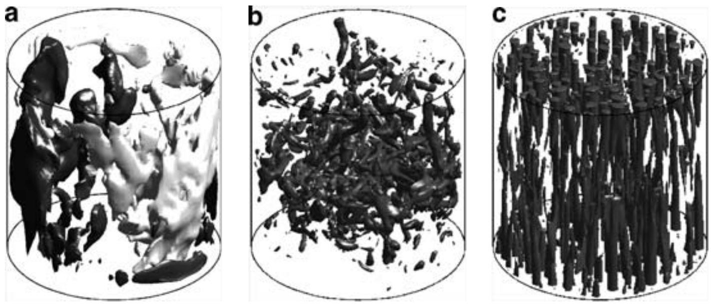

Fig. 1. (**a**) Vertical-velocity isosurfaces at $Ro = \infty$: dark (light) colouring is for upward (downward) flow. (**b**) Q isosurfaces at $Ro = 0.72$, indicating vortical regions. (**c**) Q isosurfaces at $Ro = 0.045$.

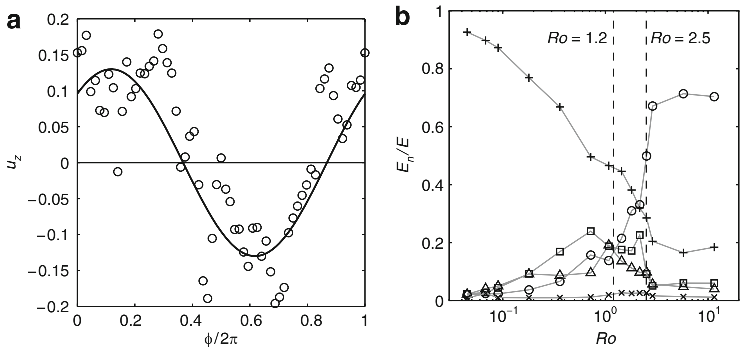

Fig. 2. (**a**) Snapshot of the azimuthal profile $u_z(\phi)$ (circles) at $Ro = 5.76$, with the corresponding $n = 1$ Fourier mode (solid line). (**b**) Averaged relative energy content E_n/E of Fourier modes: $n = 0$ (crosses), $n = 1$ (circles), $n = 2$ (squares), $n = 3$ (triangles) and the sum of modes $n \geq 4$ (pluses). The vertical dashed lines indicate $Ro = 1.2$ and 2.5.

columnar vortices are found, stretching vertically across the domain. A quasi-two-dimensional bulk state is achieved, with boundary layers to connect to the solid walls. The vertical transport of fluid and heat is confined within the vertical tubes. Statistics concerning the number and size of the vortices are presented elsewhere [8].

While such visualisations may aid in the detection of an LSC or vortices, we also define a quantitative criterion for presence of an LSC. A procedure used by Brown and Ahlers [1] is followed. We fit sinusoidal functions to the axial velocity as recorded by the numerical probes using a Fourier transform in the azimuthal direction. The average energy content E_n of each Fourier mode n can then be determined, where the $n = 1$ mode can be interpreted as the 'LSC mode.' In Fig. 2a an example fit of the $n = 1$ mode is shown. Figure 2b gives the relative energy content of modes $n = 0, 1, 2, 3$ and the sum of modes $n \geq 4$. Our criterion for existence of an LSC demands that the $n = 1$ mode is the most energetic mode, i.e., E_1 is the largest contribution to the total energy E. We find that for $Ro \gtrsim 1.2$ indeed E_1 is the largest contribution and there must be an LSC, while at $Ro \lesssim 1.2$ more and more of the energy is found in the higher-n modes, corresponding to smaller and smaller flow structures (the narrow vortical tubes). There is a rather narrow transition region $1.2 \lesssim Ro \lesssim 2.5$ in which the strength of the $n = 1$ mode (the LSC) is smaller than at larger Ro, but still the largest individual mode.

4 Heat transfer

The dependence of Nu on Ro is shown in Fig. 3, depicted as $Nu(Ro)$ normalised by its non-rotating value $Nu(Ro = \infty)$. Results from other numerical [13] and experimental [6, 14] studies are also included. Remarkable is the 15% *increase* of Nu at $Ro \approx 0.2$ in the current results (squares). Thus, despite the increased stability under rotation [9] the convective heat transfer is *larger* for a range of Ro. All other included results indicate that heat transfer can be increased by rotation, but the peak heat flux is not at a uniform Ro value. A considerable dependence on the parameters (Ra, σ, Γ) is expected.

In the current work, the increased heat transfer is found only when the LSC is absent according to the criterion mentioned before. The vortical state is thus able to transport more heat. The so-called Ekman pumping [15], occurring when a vortex connects to a solid wall in rotating flows, provides a means of entraining fluid from very close to the walls into the vortices, that subsequently transport this fluid to the other side. This mechanism is considered responsible for the increase of Nu observed in Fig. 3. At $Ro < 0.2$, however, the stabilising effect of rotation takes precedence and Nu is reduced.

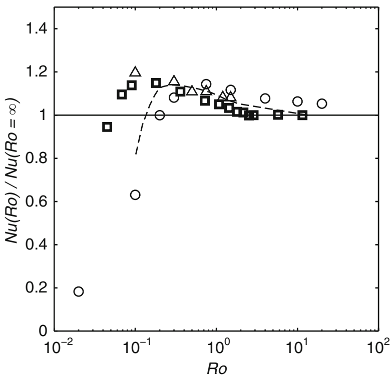

Fig. 3. Normalised heat transfer $Nu(Ro)/Nu(Ro = \infty)$ as a function of Ro. Squares: current results ($Ra = 10^9$, $\sigma = 6.4$, $\Gamma = 1$). Circles: $Ra = 2 \times 10^8$, $\sigma = 0.7$, $\Gamma = 0.5$ [13]. Triangles: $Ra = 10^9$, $\sigma = 6.3$, $\Gamma = 0.78$ [6]. Dashed line: $Ra = 2.5 \times 10^6$, $\sigma = 6.8$, $\Gamma > 6$ [14].

5 Concluding remarks

Convection in a rotating cylinder displays various types of flow-structuring, dependent on the rotation rate. The LSC is found for zero and small rotation, while at higher rotation rates many vortical structures can be observed. The organisation of the flow into coherent structures has important consequences for the heat transfer. There is a peak heat transfer at a Rossby number for which no LSC is formed. The vortical plumes, rather than the LSC, are involved in the increased heat transfer through Ekman pumping. The stabilising effect of rotation is felt at the lowest Rossby number used in this work. At even lower Rossby numbers the rapid reduction of the heat transfer is expected to continue. The boundary-layer regions are currently under investigation. We wish to quantitatively describe the Ekman pumping, to improve our understanding of the changes in the heat flux under rotation. The analysis will also shed more light on what triggers the 'destruction' of the LSC.

Acknowledgements

RPJK wishes to thank the Foundation for Fundamental Research on Matter (FOM) for financial support. This work was sponsored by the National Computing Facilities Foundation (NCF) for the use of supercomputer facilities, with financial support from the Netherlands Organisation for Scientific Research (NWO).

References

1. Brown E, Ahlers G (2006) J Fluid Mech 568:351–386
2. Xi HD, Zhou Q, Xia K-Q (2006) Phys Rev E 73:056312
3. Grossmann S, Lohse D (2000) J Fluid Mech 407:27–56
4. Hart JE, Kittelman S, Ohlsen DR (2002) Phys Fluids 14:955–962
5. Sakai S (1997) J Fluid Mech 333:85–95
6. Liu Y, Ecke RE (1997) Phys Rev Lett 79:2257–2260
7. Kunnen RPJ, Clercx HJH, Geurts BJ (2006) Phys Rev E 74:056306
8. Kunnen RPJ (2008) Turbulent rotating convection. PhD Thesis, Eindhoven University of Technology, Eindhoven
9. Chandrasekhar S (1961) Hydrodynamic and Hydromagnetic Stability. Oxford University Press, Oxford
10. Verzicco R, Camussi R (2003) J Fluid Mech 477:19–49
11. Verzicco R, Orlandi P (1996) J Comput Phys 123:402–414
12. Haller G (2005) J Fluid Mech 525:1–26
13. Oresta P, Stringano G, Verzicco R (2007) Eur J Mech B/Fluids 26:1–14
14. Rossby HT (1969) J Fluid Mech 36:309–335
15. Gill AE (1982) Atmosphere-Ocean Dynamics. Academic Press, London